University of Padua
Faculty of Engineering

Graduation Thesis
submitted for the degree of
Information Engineering

Compressed Sensing and Fluorescence Microscopy

Student:
Chiara Bizzotto
611032

Supervisor:
Prof. Dr Michele Pavon

24th September 2012

Academic Year 2011/2012

Contents

Introduction

The main purpose of my work is to report an alternative way to see the process of data acquisition: why is necessary, in the transition between analog and digital, to keep all data if then one has to compress it to save memory as much as possible? And if one wants to apply this hypothesis, for example in Fluorescence Microscopy, what are the outcomes?

A solution to this apparent contradiction is found in the technique of *Compressed Sensing*: to introduce the topic I've started with the description of the *Fourier Transform*, whose coefficients are a valid representation of most signals. In particular, I've presented the *Discrete Fourier Transform* and the *Dscrete-Time Fourier Transform* because most of the signals we deal with have discrete values.

Subsequently in Chapter 2 I've dealt with *Sampling Theory*, the principal approach to data acquisition used before the introduction of *Compressed Sensing Theory* and which is mainly based on *Shannon's Theorem*. Under the hypotheses of the Theorem, one can reduce the number of measurements but it is evident that there's more that can be done about it.

Finally one can find in Chapter 3 a concise but sufficient treatment of *Compressed Sensing* in which I've especially underlined the importance of *sparsity* and *incoherence* as requirements for signals recovery.

In conclusion I've described some examples of biological images acquisition through a *Compressive Fluorescence Microscope* which show how a practical implementation of the theory can considerably reduce the number of necessary measurements.

Chapter 1

DFT e DTFT

1.1 Discrete Fourier Transform (DFT)

Before we talk specifically about the DFT, let's take a look in general at the *Fourier Transform (FT)* of a continuous-time signal. Given a finite-energy signal x ($x \in L^2(-\infty, \infty)$, it may be defined as a mean-square limit.

$$X(\omega) = \int_{-\infty}^{+\infty} x(t)e^{-j\omega t}dt, \qquad \omega \in (-\infty, +\infty) \tag{1.1}$$

As we know from Signal Theory, the passage from *continuous time* to *discrete*, is marked by the use of the sum instead of the integral, and therefore we have:

$$X(\omega_k) = \sum_{n=0}^{N-1} x(t_n)e^{-j\omega_k t_n}, \qquad k = 0, 1, 2, ..., N-1 \tag{1.2}$$

where $x(t_n)$ is the input signal amplitude at the sampling time $t_n =$ and N is the number of time and frequency samples.

Because the sampling period T is also written as $T = \frac{2\pi}{\omega_k}$ and it's commonly set at 1, (1.2) becomes:

$$X(k) = \sum_{n=0}^{N-1} x(n)e^{-jn\frac{2\pi}{N}k}, \qquad k = 0, 1, 2, ..., N-1 \tag{1.3}$$

where $e^{j2\pi nk/N} = s_k(n)$ is the sampled complex sinusoid and n is the new variable for the discrete time. It's now easy to see that $X(k)$ is the inner product of x and s_k,

$$X(k) = \langle x, s_k \rangle = \sum_{n=0}^{N-1} x(n)\overline{s_k(n)} \tag{1.4}$$

Therefore the DTF is a measure of "how much" of the *basis sinusoid* s_k is present in x and at what phase.

1.2 Discrete Time Fourier Transform (DTFT)

The *Discrete Time Fourier Transform* is the limiting form of the DFT (1.3) when $N \to +\infty$:

$$X(e^{j\theta}) = \sum_{n=-\infty}^{\infty} x(n)e^{-j\theta n} \qquad x \in \ell^2(-\infty, \infty) \tag{1.5}$$

Differently from the DFT, which involves only a finite number N of samples of the signal, the $DTFT$ operates on discrete-time signals $x(n)$ which are defined over all integers $n \in \mathbb{Z}$.

We see that the $DTFT$ is a function of continuous frequencies $\theta \in [-\pi, \pi]$, contrary to the DFT whose frequencies $\omega_k = 2\pi k/N$ $(k = 0, 1, 2, ..., N-1)$ are discrete and are obtained by the angles of N points along the unit circle in $\mathbb{C}$. When $N \to \infty$, the frequency axis form the unit circle and remains finite in length in accordance with the time domain which is sampled.

Given the discrete-time signal $x(n)$ with $n \in \mathbb{Z}$ and $x(n) \neq 0$ only for n=0,1,...,N-1, let's $x_p(n)$ be the periodic repetition of period N of x. Its Fourier series is

$$x_p(n) = \sum_{k=0}^{N-1} a_k e^{jk\frac{2\pi}{N}n} \tag{1.6}$$

and from this we derive a_k as:

$$a_k = \frac{1}{N} \sum_{n=0}^{N-1} x_p(n)e^{-jn\frac{2\pi}{N}k} \tag{1.7}$$

From (1.7) and (1.3) we see that:

$$\begin{pmatrix} x(0) \\ x(1) \\ \cdot \\ \cdot \\ x(N-1) \end{pmatrix} \overset{DFT}{\longmapsto} N \begin{pmatrix} a_0 \\ a_1 \\ \cdot \\ \cdot \\ a_{N-1} \end{pmatrix}$$

Therefore we can write the DFT of $x_p(n)$ as:

$$\tilde{X}(k) = Na_k = X(e^{j(k\frac{2\pi}{N})}) \tag{1.8}$$

We see that $\tilde{X}(k)$ is nothing but samples of the $DTFT$ (1.5).

Chapter 2

Sampling Theory

The discrete-time signal $x(n)$ is often the sampled version of a continuous-time signal $x(t)$ at time $t_n = nT$, where T is the sampling period. On account of this the $DTFT$ can be seen as an approximation of the continuous-time Fourier Transform

$$X(j\omega) = \int_{-\infty}^{\infty} x(t)e^{-j2\pi\omega t}dt \tag{2.1}$$

Hence the question is: can we determine from the samples $\{x(nT)\}$ the $DTFT$ $X(j\omega) = \mathcal{F}\{x(t)\}$ and therefore, the original signal $x(t)$? How good is this approximation? An answer to this question is given to us by "*Shannon's Sampling Theorem*":

Theorem 1. (Shannon's Sampling Theorem) *If* $\exists\ \omega_M$ *(Nyquist rate) such that* $X(j\omega) = \mathcal{F}\{x(t)\} = 0\ \forall\ |\omega| > \omega_M$ *and if* $\omega_S = \frac{2\pi}{T} > 2\omega_M$*, then we can reconstruct x(t) in the mean-square sense from its samples* $x_P(t) = x(nT)$*.*

Thus if we have an image, the sampling frequency ω_S, that is the inverse of the image size in pixels, must be at least twice the bandwidth of the signal ω_M. This procedure of picture capture is obviously independent from the image type and from this perspective we can do something to reduce the number of samples without compromising the data.

For example if we have a signal $x(t)$, we obtain its discrete version through a series of impulses $p(t) = \sum_{n=-\infty}^{\infty} \delta(t - nT)$, where $T = \frac{2\pi}{\omega_S}$ is the period:

$$x_P(t) = x(t)p(t) = x(t) \sum_{n=-\infty}^{\infty} \delta(t - nT) = \sum_{n=-\infty}^{\infty} x(nT)\delta(t - nT) \tag{2.2}$$

From $P(i\omega) = \mathcal{F}\{p(t)\} = \frac{2\pi}{T} \sum_{k=-\infty}^{\infty} \delta(\omega - k\omega_S)$, we calculate $\mathcal{F}\{x_P(t)\}$:

$$X_P(j\omega) = \frac{1}{2\pi}\int_{-\infty}^{\infty} X(j\theta)P(j(\omega-\theta))d\theta = \frac{1}{T}\sum_{k=-\infty}^{\infty} X(j(\omega-k\omega_S)) \quad (2.3)$$

which is periodic of period ω_S.

In (2.3) to calculate $X_P(j\omega)$ we have used the property of the Fourier Transform:

$$\mathcal{F}\{x(t)y(t)\} = \frac{1}{2\pi}X(j\omega) * Y(j\omega)$$

and then the one of the delta function:

$$X(j\omega) * \delta(\omega-\omega_O) = X(j(\omega-\omega_O))$$

Example of sampling without aliasing

Let's take into account a real signal $x(t)$ with the following Fourier Transform $X(j\omega)$

Figure 2.1: $|X(j\omega)|$

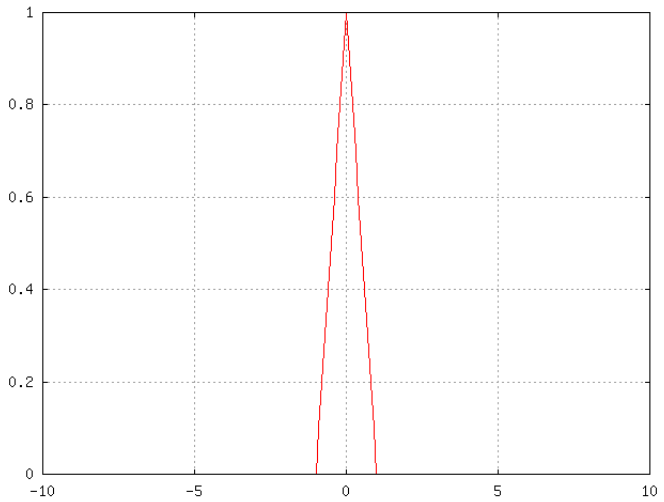

We see that the signal is limited in frequency, namely $X(j\omega) = 0 \; \forall \; |\omega| \geq B = 1$, therefore $\omega \in (-1, 1)$.

To avoid aliasing, which leads to data loss or distortion, we have to use a sampling rate $\omega_S \geq 2B = 2$.
We consider $\omega_S = 5$ and so we obtain $X_P(j\omega)$ (fig. 2.2).

Figure 2.2: $|X_P(j\omega)|$

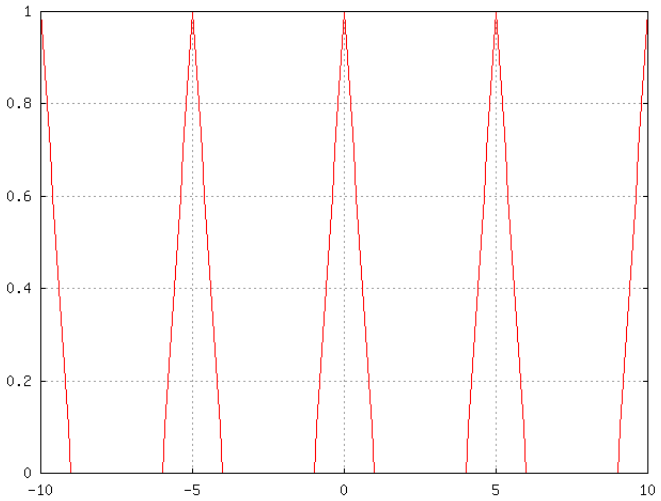

To obtain the original signal we have to return to the original transform $X(j\omega)$ removing the spectral repetition introduced by the sampling. To achieve this, we can use an ideal low-pass filter (fig. 2.3)

Figure 2.3: $|H(j\omega)|$

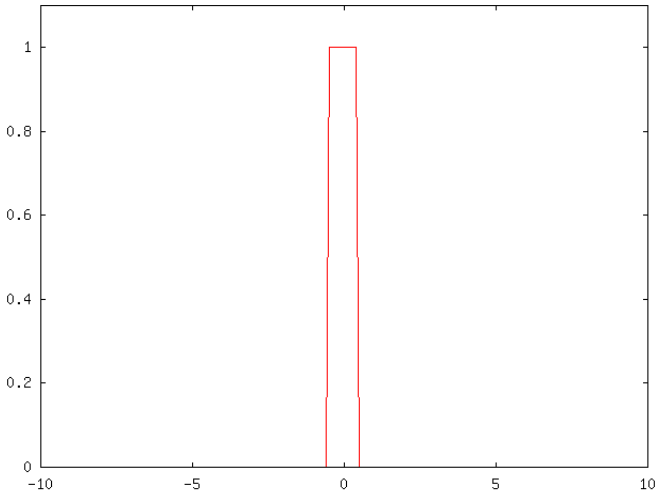

$$H(j\omega) = Trect\left(\frac{\omega}{\omega_S}\right) = \begin{cases} T & |\omega| < B \\ T/2 & \omega = \pm B \\ 0 & \text{altrove} \end{cases}$$

From $H(j\omega)$ we obtain $X_r(j\omega) = X_P(j\omega)H(j\omega)$ that is a reconstructed version of $X(j\omega)$, which, in this case, according to Shannon's Theorem (Theorem 1), coincides with the original one $X(j\omega)$.

Example of sampling with aliasing

On the contrary, if the sampling frequency ω_S doesn't respect the Shannon's Theorem (Theorem 1), there's the risk that the reconstructed signal presents the aliasing phenomenon, namely during the sampling the translates of the signal transform overlap with each other.
For example, if in the previous case we use $\omega_S = 1,8 < 2B = 2$, we would have the following results for the $X_P(j\omega)$ (fig. 2.4).

Figure 2.4: $|X_P(j\omega)|$

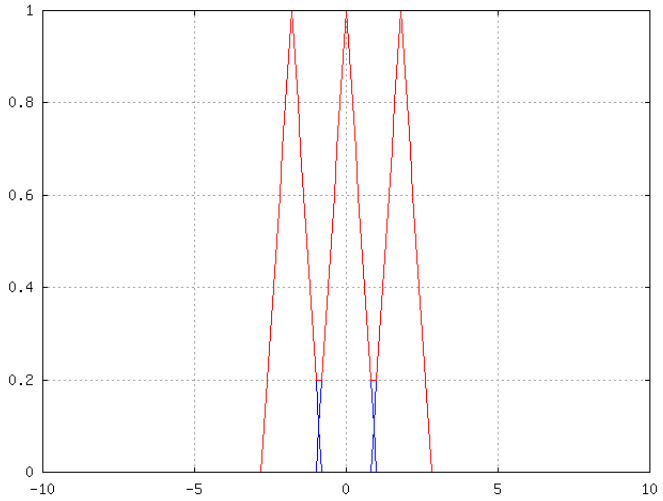

Due to the overlaps the reconstructed signal $X_r(j\omega)$ would be, in this case, different from $X(j\omega)$.

Chapter 3

Compressed Sensing

Nowadays we deal with data that are compressed, either if we talk about music (.mp3, .aac,...) or videos (.avi, .mp4, ...) or images (.jpg, .gif,...). As a matter of fact all these signals have some data that would be cut off during compression without severe damage to the outcome and that are therefore 'useless', in the meaning that they are acquired only to be later thrown out.

The idea behind *Compressed Sensing* is that, for a picture, we can directly acquire only the information that is useful, without knowing where it is located in the image.

In this sensing mechanism, information about the signal $x(t)$ is obtained by linear functionals:

$$y_k = \langle x, \varphi_k \rangle, \qquad k = 1, ..., m \tag{3.1}$$

The equation shows a correlation between the signal we want to acquire and the sensing waveforms $\varphi_k(t)$: for example if $\varphi_k(t) = \delta(t-k)$, then $\mathbf{y}$ is simply a vector of sampled values of $\mathbf{x}$, or if the sensing waveforms are sinusoids, then $\mathbf{y}$ contains the Fourier coefficients.

Compressed Sensing is only interested in undersampled problems, that is when the number m of samples is smaller than the dimension n of the signal $\mathbf{x}$. Therefore we have to solve an underdetermined linear system of equations with more unknowns than equations.

As we saw in the previous chapter (Theorem 1), if $x(t)$ has very large bandwidth, we need a small number of uniform samples to recover the signal. As we will see in this chapter, *Compressed Sensing* makes the recovery possible for a broader class of signals under some peculiar features: sparsity and incoherence.

Sparsity

Many natural signals are sparse in the sense that their "information content" is much smaller than suggested by their bandwidth. Therefore their representation could be more concise if expressed in a proper basis.

If we have a signal $x(t)$, it may be represented through an expansion in an orthonormal basis $\Psi = [\psi_1 \psi_2 ... \psi_n]$ as follows:

$$x(t) = \sum_{i=1}^{n} \alpha_i \psi_i(t) \tag{3.2}$$

where $\alpha_i = \langle x, \psi_i \rangle$ are the coefficients of x.
Hence a signal is sparse if one can discard the small coefficients without much sensible loss. We name $x_S(t)$ the signal obtained keeping only the terms corresponding to the S largest value of α_i so that (3.2) becomes:

$$x_s(t) = \sum_{k=1}^{S} \alpha_k^S \psi_k \tag{3.3}$$

where α_i^S are the S largest coefficients.
Since Ψ is an orthonormal basis, $\|\mathbf{x} - \mathbf{x_S}\|_{\ell_2} = \|\alpha - \alpha_{\mathbf{S}}\|_{\ell_2}$ and if x is sparse then α is well approximated by $\alpha_{\mathbf{S}}$ and hence the error $\|\mathbf{x} - \mathbf{x_S}\|_{\ell_2}$ is small.

The real advantage that sparsity brings to *Compressed Sensing*, is that one can efficiently acquire signals nonadaptively, namely in a way that doesn't require the knowledge of all the n coefficients α_i to determine the significant S ones.

Incoherence

Another peculiar feature of the signal required by CS is incoherence: while the signal of interest has to be sparse in Ψ, on the contrary the sampling waveforms have to be very dense in Ψ.

Let's consider two orthonormal basis of $\mathbb{R}^n$, $\langle \Phi, \Psi \rangle$, where Φ is used to sense the signal x as in (3.1) and Ψ to represent $\mathbf{x}$: we can define coherence between Φ and Ψ as follow:

$$\mu(\Phi, \Psi) = \sqrt{n} \max_{1 \leq k,h \leq n} |\langle \varphi_k, \psi_h \rangle| \tag{3.4}$$

It's now clear that the coherence is related to the correlation between Φ and Ψ: if Φ and Ψ contain correlated elements, μ is going to be large ($\mu(\Phi, \Psi) \in [1, \sqrt{n}]$).

For example if Φ is the canonical basis with $\varphi_k(t) = \delta(t-k)$ and Ψ is the Fourier basis with $\psi_h(t) = n^{-1/2} e^{j2\pi ht/n}$, we have $\mu(\Phi, \Psi) = 1$ and therefore maximal incoherence. Or if we create an orthonormal basis Φ at random, orthonormalizing n vectors sampled independently and uniformly on the unit sphere, then with a probability close to one, $\mu(\Phi, \Psi) = \sqrt{2 \log n}$.

3.1 Signal Recovery

The goal of this technique is to recover signals from only m of the n available coefficients ($m < n$). We use ℓ_1-norm minimization with $\|\alpha\|_{\ell_1} = \sum_i |\alpha_i|$:

$$\min_{\tilde{\alpha} \in \mathbb{R}^n} \|\tilde{\alpha}\|_{\ell_1} \text{ subject to } y_k = \langle \varphi_k, \Psi\tilde{\alpha} \rangle \tag{3.5}$$

where $\Psi\tilde{\alpha} = \mathbf{x}$ and Ψ is the $n \times n$ matrix with $\psi_1, ..., \psi_n$ as columns.

One can think to recover the signal via ℓ_2-norm minimization, that is searching the $\tilde{\mathbf{x}}$ with minimal energy, but this system doesn't allow us to obtain S-sparse solutions and as we can see in Figure 3.1 the reconstruction is not exact. We run into a similar problem if we use the ℓ_0-norm that gives us S-sparse solutions but it requires all the possible positions of the S nonzero coefficients.

Thus the reconstructed signal is given through the ℓ_1-norm minimization by

$$\mathbf{x}^* = \Psi\alpha^* \tag{3.6}$$

where α^* are the coefficients according to (3.5), namely among all possible $\tilde{\mathbf{x}} = \Psi\tilde{\alpha}$, we choose the one $\mathbf{x}^*$ which has minimal $\|\alpha\|_{\ell_1}$.

If $\mathbf{x}$ is sparse with a probability close to one, $\mathbf{x}^* = \mathbf{x}$, that is the recovery is exact.

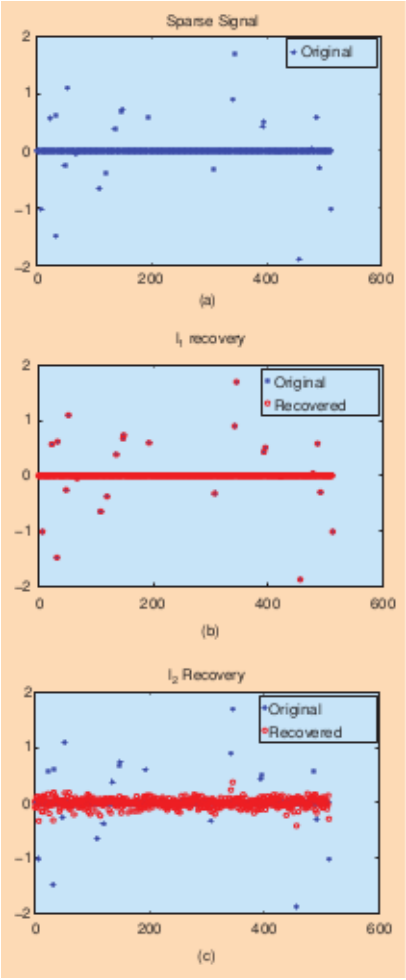

Figure 3.1: Example of signal recovery: (a) sparse real valued signal, (b) its reconstruction by ℓ_1 minimization and (c) its reconstruction by ℓ_2 minimization

Theorem 2. *Given* $\boldsymbol{x} \in \mathbb{R}^n$ *supposed S-sparse in* Ψ *and chosen* m *measurements in* Φ *uniformly at random, then if*

$$m \geq C\mu^2(\Phi, \Psi) S \log n \quad C > 0,$$

the solution to (3.5) $\mathbf{x}^*$ *is exact with large probability.*

We clearly see the big role played by coherence in Theorem 2: the smaller is the coherence, the smaller the number of needed samples m becomes. In fact if μ is close to one, then m is on the order of $S \log n$. The ℓ_1-norm minimization technique allows to recover a signal $\mathbf{x}$ without any knowledge about the number of relevant coefficients α_i^*, their locations among all the n coefficients $\tilde{\alpha}_i$ or their amplitude, that is we can acquire signals *nonadaptively.*

Also sparsity is crucial but we have to be careful: there are indeed some sparse signals that are zero nearly everywhere in Φ, that is almost all $y_k = \langle x, \varphi_k \rangle = 0$ for all $k = 1, ..., m$. In this situation one would have a stream of zeros and it would be impossible to reconstruct the signal. Therefore we don't need more than $O(S \log n)$ samples but we can't recover the signal if they are less.

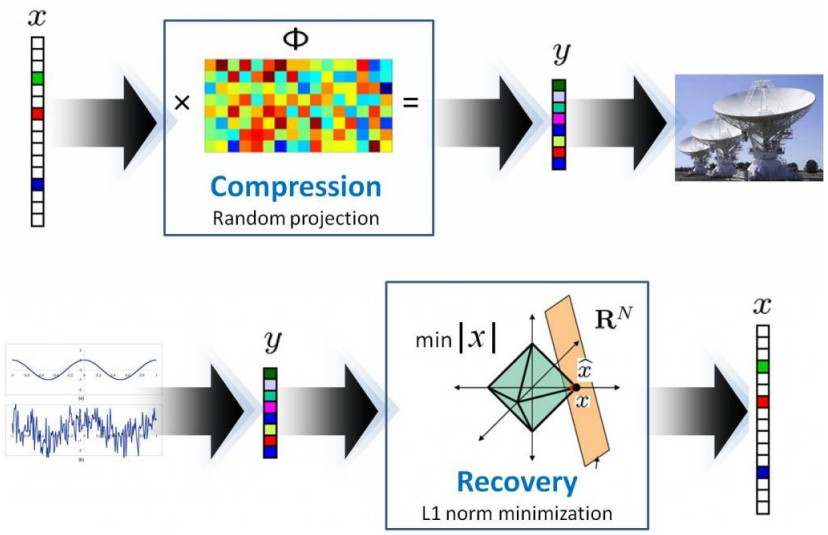

Figure 3.2: Illustration of compressed sensing

The important goal that *Compressed sensing* allows us to achieve, is that one can directly acquire only the important information about an object, namely that which would remain after compression.

Chapter 4

Fluorescence Microscopy

The fluorescence microscope is becoming an essential tool in biology and medical sciences and this is because it has some peculiar features that are not available in conventional microscopes. Contrary to the traditional optical one, the fluorescence microscope uses a much more intense light that excites the fluorescent species in the object: besides the magnified image is based on the light emanating from the specimens rather than the light used to illuminate the sample. The interesting side of this technic is that one can use it not only with autofluorescent specimens, but also with added fluorochromes, which are excited by specific wavelenghts of light.

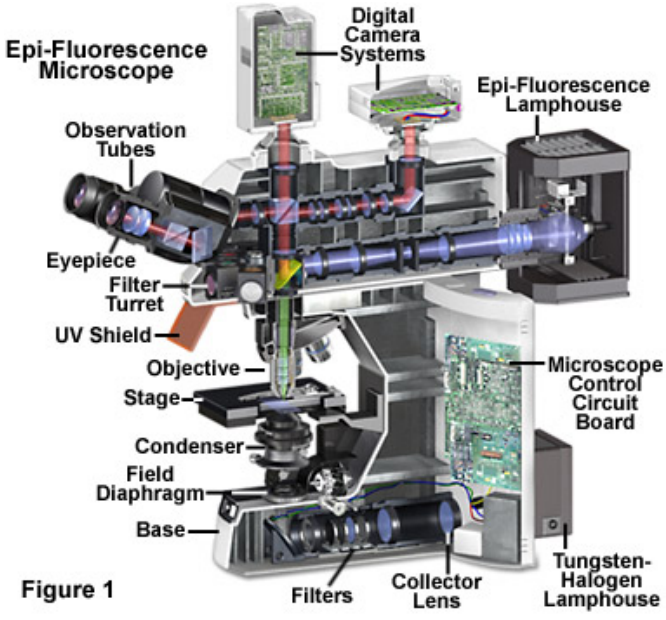

Figure 4.1: Example of an Epi-Fluorescence Microscope

To acquire the image, the specimen is illuminated with a specific band of wavelengths: only the emission light should reach the detector so that the outcome is a bright image against a dark background. To achieve that the weaker emitted fluorescence should be blocked.

The light of a specific wavelength is produced by passing multispectral light through a wavelength selective filter. The light passed by the filter reflects from the surface of a dichromatic mirror through the objective to illuminate the specimen. The light emitted by the fluorescent specimen passes back through the dichromatic mirror and is filtered by an emission filter, which blocks the unwanted wavelengths, though most of the excitation light reaching the dichromatic mirror is reflected back toward the light source.

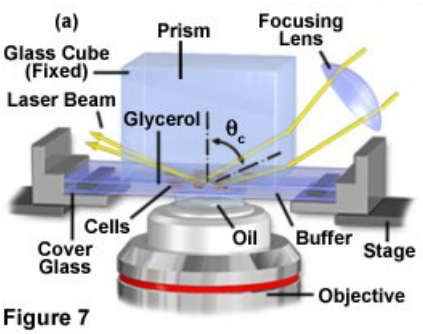

Figure 4.2: Inverted Microscope TIRFM

The only factor that could compromise the outcome is the presence of the optical background noise even if it's minimal: it is caused also by the microscope itself because of the autofluorescence of the material and therefore it would seem inevitable. Total internal reflection fluorescence microscopy (TIRFM) takes advantage of the evanescent wave, that is produced when light is totally internally reflected at the interface between two media with different refractive indices, and provides the optimal combination of low background and high excitation light.

A beam of light (usually laser) is directed through a prism of high refractive index which borders on a lower refractive index medium: if the direction of the light has an angle that is higher than the critical one, the beam will be totally internally reflected at the interface. This phenomenon produces an evanescent wave at the interface thanks to the generation of an electromagnetic field that goes 200 nanometers or less into the lower refractive index medium. The light intensity of this wave is high enough to excite the fluorophores in the specimen even if very little of it is exposed: this leads to a low background noise as wanted.

4.1 Compressive Fluorescence Microscopy

For the experiments it was used a standard epi-fluorescence inverted microscope (Nikon Ti-E) as shown in Figure 4.3: it was also added a Digital Micromirror Device (DMD) to generate spatially modulated excitation patterns. The DMD is a 1024-by-768 array of micromirrors that can be shifted between two orientations, +12° and -12° with respect to the surface, and is positioned so that the optical axis is orthogonal to the plane of the DMD.

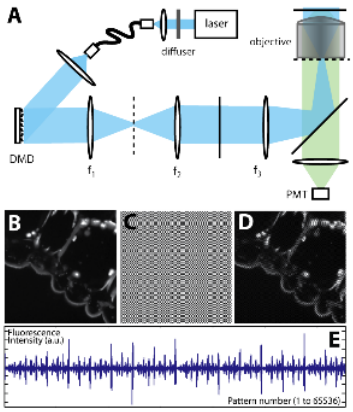

Figure 4.3: (a) Experimental set-up, (b) Slice of lily anther, (c) Projection of a Hadamard pattern on a uniform fluorescent pattern, (d) Projection of the pattern on the biological sample, (e) Fluorescent intensity during acquisition sequence.

The laser beam passes first through a diffuser to reduce spatial coherence and then it's coupled to a multimode fiber. The beam is then expanded into a 2cm diameter beam and oriented towards the DMD at an angle of incidence that is twice the tilting angles of the DMD mirrors: micromirrors oriented at +12° reflect the light and appear as bright pixels in the sample plane, while micromirrors oriented at -12° appear as dark pixels. Depending of the sample one can use different objectives (air or oil-immersion) and according to this the imaging lenses (f_1, f_2 and f_3 in Figure 4.3) introduce different reduction: 1,5X for the air-immersion objective and 1X for the oil-immersion one. The fluorescence emanated by the specimen is detected on a photomultipler tube PMT and sampled at 96kHz using an analog-digital converter board. In *Compressed Sensing* measurements, the information on the sample is given by the variations of the intensity as in Figure 4.3 (e).

One of the crucial points, as seen in the previous chapters, is to determine the basis Φ which should be as incoherent as possible with the basis Ψ of the signal, even if we have no information about it. The choice falls into the Hadamard system which is known to be highly incoherent with the basis in which most natural signals are sparse, for example with the Dirac basis.
A Hadamard basis can be identified with a matrix $n \times n$ (with $n = 2^k$) whose entries are $h_{jk} \in \{+1, -1\}$ and which rows are mutually orthogonal.
For example if we have

$$H_2 = \begin{pmatrix} 1 & 1 \\ 1 & -1 \end{pmatrix}, \quad \text{then} \quad H_4 = \begin{pmatrix} 1 & 1 & 1 & 1 \\ 1 & -1 & 1 & -1 \\ 1 & 1 & -1 & -1 \\ 1 & -1 & -1 & 1 \end{pmatrix} \tag{4.1}$$

and in general all $H_{2\ell}$ can be constructed by recursion:

$$H_{2\ell} = \begin{pmatrix} H_\ell & H_\ell \\ H_\ell & -H_\ell \end{pmatrix} \tag{4.2}$$

Since the excitation pattern is generated by the micromirrors, every $\varphi_i[k]$ can be either 1 or 0 and we have to redefine φ_i as a shifted and rescaled version of h_i: φ_i=(h_i+1)/2. The sensing function φ represents light intensities and its components are thus non-negative.
From the recording of the fluorescence intensity we have to recover the signal x by solving the optimization problem (3.5) and because the measurements are noisy it becomes:

$$\min_{\mathbf{x}\in\mathbb{R}^n} \|\Psi^T\mathbf{x}\|_{\ell_1} \qquad \text{subject to} \qquad \|\mathbf{y}-\Phi\mathbf{x}\|_{\ell_2} \leq \epsilon \tag{4.3}$$

where Ψ^T is the transposed of Ψ with $\psi_1, ..., \psi_n$ as rows.
For computational reasons one can solve instead a relaxed version of the problem:

$$\min_{\mathbf{x}\in\mathbb{R}^n} \|\Psi^T\mathbf{x}\|_{\ell_1} + \frac{\gamma}{2}\|\mathbf{y}-\Phi\mathbf{x}\|_{\ell_2}^2 \tag{4.4}$$

where γ is a parameter that depends on ϵ.

4.2 Experiments

4.2.1 Fluorescent beads

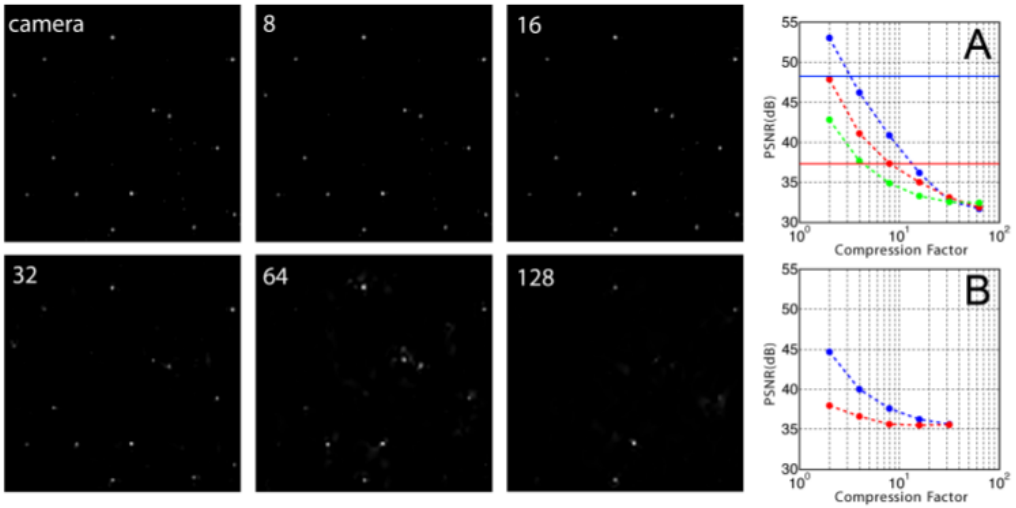

Figure 4.4: Camera snapshot and reconstructed bead images with undersampling ratio equal to 8, 16, 32, 64 and 128; (a) plot of the PSNR of the simulated data for a nominal illumination level (blue), for the same level reduced by a factor 10 (red) and by a factor 100 (green); (b) same as (a) for the experimental data

First we try to acquire an image of fluorescent beads (diameter 2μm, peak emission at 520nm, Fluorospheres Invitrogen) which appears as few bright spots in a dark background. As Ψ, one can equally use either the Dirac basis or a wavelet transform, but in this case it was used the wavelet transform with 512 random 256×256 Hadamard patterns. After defining the *Undersampling ratio* as the ratio between the number n of pixels and the number m of measurements, we see that in this case it can be up to 64, namely 1 measurement every 64 pixels is enough, and the signal would still be recovered. With a higher undersampling ratio a lot of beads, expecially the ones with low intensity, are lost.

An approximation of the distortion of the recovered image is given by the Peak Signal-to-Noise Ratio (PNSR), which we define as follow:

$$PNSR = 10 \log \frac{d^2}{MSE} \qquad \text{with} \qquad MSE = \frac{1}{n}\|\mathbf{x} - \mathbf{x}^*\|_{\ell_2}^2 \tag{4.5}$$

where $\mathbf{x}^*$ is the reconstructed signal from m measurements and d is the dynamical range of the reconstruction obtained from a full sample.

As we see in Figure 4.4 A, the PSNR decreases with the undersampling ratio and reaches a plateau at 64, but it depends also on the illumination: since low-intensity beads are lost before bright ones, measurements have been repeated with an excitation light intensity reduced by a factor 100 (green curve) and, as expected, the PSNR is lower and reaches a plateau at an undersampling ratio of 10 where however almost all beads are lost.

Another aspect that we have to take into consideration is the presence of photon noise that at these low intensities could play an important role in the distortion of the reconstructed image. To achieve that, the measurements are repeated again on an artificial image of fluorescent beads made of 50 spots randomly positioned in the 256×256 pixels. The reconstructions take place with intensities I_0, $I_0/10$ and $I_0/100$ with undersampling ratios between 2 and 64. As we can see in Figure 4.4 B there is a decrease of efficiency for low-light levels but one can not quantitatively estimate the PSNR of the reconstructed image up to a ratio equal to 64. This suggests that photon noise isn't the only source of image degradation.

4.2.2 Lily anther slice

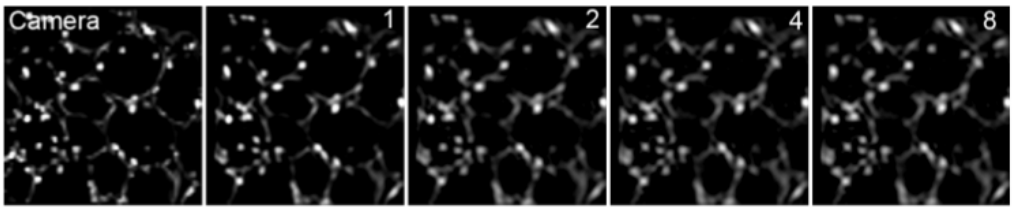

Figure 4.5: Image of a slice of lily anther and, from left to right, the reconstructed image with undersampling ratios between 1 and 8

The second acquisition is of a slice of lily anther sampled with 128×128 Hadamard pattern: as basis Ψ it's used the Curvelet Transform because it's known that contour-like pictures are sparse in it.

In this case we can reconstruct the image up to an undersampling ratio of 8: the fact that it's not so high as for the beads, can be explained by the lesser sparsity of the image. Furthermore this sample is not properly two dimensional because of the thickness of the slice (about 50μm) and this interferes with the image reconstruction.

4.2.3 Zyxin-mEOS2 COS7 cells

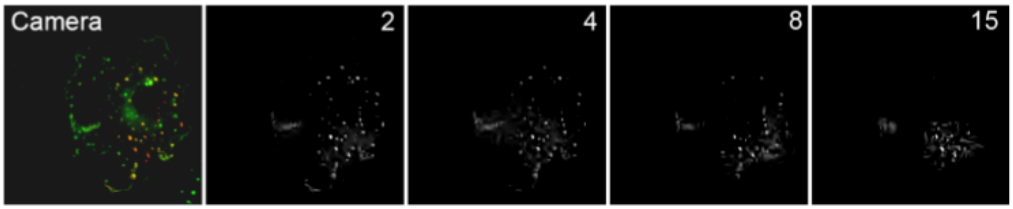

Figure 4.6: Image of COS7 cells expressing Zyxin-mEOS2 with superposition of the conventional epifluorescence image of the native (green) and converted form (red) and, from left to right, the reconstructed image with undersampling ratios equal to 2, 4, 8 and 15

In many biological applications we deal with high magnification and high NA optics[1] which leads to a limitation due to the short focal depth. Therefore in these conditions (oil-immersion objective and NA equal to 1,45), photoactivation techiques were used on the specimens: COS7 cells were transfected with Zyxin-mEOS2, which is a focal adhesion protein, at the surface on which the cells are plated, fused with a genetically-encoded photoconvertible fluorescent protein tag that has normally green fluorescence and red one if illuminated with violet light. For the acquisition a wavelet transform was used as sparsity basis Ψ and 32768 different Hadamard patterns: even if the emitted fluorescence of the cells is low, the reconstruction is good for undersampling ratios up to 8 and tends to degrade at a ratio equal to 15. Also in this case the photon noise due to the low illumination is a limiting factor for CS imaging.

[1]NA is a parameter that characterizes the range of angles over which the system can accept or emit light. It's directly proportional to the index of refraction of the medium in which the lens is located and to the half-angle of the maximum cone of light that can enter or exit the lens.

Conclusions

The main goal of the modern society is to save money and resources in every possible area and Information Engineering makes no exception: for a long time it focused on the compression of data to save space on the storage devices and only recently it began to get to the root of the problem by trying to intervene during data acquisition.
We saw that we can reduce the number of the needed samples thanks to *Shannon's Theorem* but with a very restrictive condition: the signal must have a limited bandwidth ω_M and, because the number of measurements is proportional to ω_M, it has to be also very narrow to have a concrete reduction of the measurements number.

With the *Compressed Sensing* technique instead, one can transform analog data into an already compressed digital form, through very few measurements, without losing information. As we have seen, one of its focal points is the possibility of 'choosing' the samples without knowing the nature of the original signal or where the important information lays: one can pick m values at random and can still reconstruct the signal. The only requirements are the sparsity of the signal in a chosen basis Φ and the incoherence of Φ with the sensing basis Ψ.

A natural step forward was to design sampling devices that directly record incoherent low-rate measurements of the analog high-bandwidth signal. An example of these devices is the *Compressive Fluorescence Microscope* which takes advantage of the natural sparsity of biological images and, combining it with the choice of a proper basis Ψ, leads to a very significant reduction of samples (up to 1/64 for the beads experiment in (4.2.1)).

The importance of *Compressed Sensing* is the fact that it has various implications in practical life, despite its being a mathematical theory: it has obvious applications in Bioengineering, Telecommunication Engineering, Robotics and Control Theory, but the strong point is its potential in everyday life like, for example, the reconstruction of noisy images and the classification of images for the automatic recognition of faces.

Bibliography

[1] Emmanuel J. Candès and Michael B. Wakin, "An introduction to Compressive Sampling" , *IEE Signal Processing Magazine*, pp. 21-30, March 2008.

[2] V. Studer, J. Bobin, M. Chahid, H. Moussavi, E. Candès and M. Dahan, "Compressive Fluorescence Microscopy for Biological and Hyperspectral Imaging", `http://www-stat.stanford.edu/~candes/`

[3] J.O. Smith, "Mathematics of the Discrete Fourier Transform (DFT) with Audio Applications", Second Edition, `https://ccrma.stanford.edu/~jos/mdft/mdft.html`, 2007, online book, accessed July 2012.

[4] Kenneth R. Spring and Michael W. Davidson, "Introduction to Fluorescence Microscopy", `http://www.microscopyu.com/articles/fluorescence/fluorescenceintro.html`